J. Membrane Biol. 123, 183–190 (1991)
002226319100118N

The Journal of
Membrane Biology

Patch-Clamp Studies on the Anomalous Mole Fraction Effect of the K^+ Channel in Cytoplasmic Droplets of *Nitella:* An Attempt to Distinguish between a Multi-Ion Single-File Pore and an Enzyme Kinetic Model with Lazy State

Silke Draber, Roland Schultze, and Ulf-Peter Hansen
Institut für Angewandte Physik, DW-2300 Kiel, Federal Republic of Germany

Summary. Patch-clamp studies have been employed in order to check whether the assumption of a multi-ion single-file pore is necessary for the explanation of the anomalous mole fraction effect or whether this effect can also be explained by a single-barrier enzyme kinetic model. Experiments in the cell-attached configuration were done on the tonoplast membrane of cytoplasmic droplets of *Nitella* in solutions containing 150 mol m^{-3} of K^+ plus Tl^+ with seven different K^+/Tl^+ ratios. At first sight, the results seem to support the multi-ion single-file pore, because apparent open channel conductivity displays the anomalous mole fraction effect, whereas open-probability has not been found to be dependent on the K^+/Tl^+ ratio. Changes in open probability would be expected for a single-barrier enzyme kinetic model with a lazy state. On the other hand, the lazy-state model is more successful in explaining the measured *I-V* curves. The entire slope of the apparent open channel current-voltage curves rotates with changing K^+/Tl^+ ratios in the whole voltage range between -100 and $+80$ mV. Numerical calculations on the basis of multi-ion single-file pores could create the anomalous mole fraction effect only in a limited voltage range with intersecting *I-V* curves. The apparent absence of an effect on open probability which is postulated by the lazy-state model can be explained if switching into and out of the lazy state is faster than can be resolved by the temporal resolution of 1 msec.

Key Words anomalous mole fraction effect · enzyme kinetic model · multi-ion single-file pore · K^+ channel · patch clamp · thallium

Introduction

In solutions containing K^+ and Tl^+ ions, a strange effect on the electric conductivity of biological membranes has been observed in starfish eggs (Hagiwara et al., 1977) and in *Chara corallina* (Tester, 1988). The conductivity decreases with increasing relative Tl^+ concentrations until a minimum is reached. If the Tl^+/K^+ ratio is increased further, conductivity goes up again. This effect is called anomalous mole fraction effect (AMFE).

Hille and Schwarz (1978) suggested that the observations of Hagiwara et al. (1977) are evidence for their multi-ion single-file pore model. According to this, Tester (1988) concluded from the observation of the anomalous mole fraction effect that the K^+ channel in *Chara,* too, can be described by the Hille-Schwarz model. However, other experiments have shown that an enzyme-kinetic model (Hansen et al., 1981) of the K^+ channel with a single energy barrier can provide a good fit of measured current-voltage curves in *Vicia faba* (Gradmann, Klieber & Hansen, 1987), in *Acetabularia* (Bertl & Gradmann, 1987), in *Chara* (Bertl, 1989) and in *Nitella* (Fisahn, Hansen & Gradmann, 1986). Curve fitting based on this model enables the determination of the charge of the transporter, of the stoichiometry of K^+ binding and of rate constants. The single-barrier enzyme kinetic model is also capable of explaining activation and deactivation processes (Hansen, Tittor & Gradmann, 1983; Hansen & Fisahn, 1987; Bertl, Klieber & Gradmann, 1988; Bertl, 1989, Hansen, 1990).

Therefore, we were interested in the question of whether the enzyme-kinetic model with a single barrier can also explain the anomalous mole fraction effect. For this purpose model calculations have been done in order to find out which configurations lead to this phenomenon. The Hille-Schwarz model as well as the single-barrier model could generate a minimum conductivity at a certain mixture of K^+ and Tl^+.

The Hille-Schwarz model starts from the assumption of a rigid pore with several binding sites for the permeant ion which are separated by energy barriers (*see* Fig. 6*A*). Transport can be described by transitions between different states which are characterized by the occupation of the binding sites (see Fig. 6*B*). The model of Hansen et al. (1981, 1983) also applies to a pore with energy barriers.

However, in all curve-fitting approaches done so far, it was sufficient to assume one single energy barrier. This is not a crucial difference, and additional barriers may be incorporated if required by experimental data. More important is the assumption of a recycling step. After release of an ion at one side, a conformational change of the protein has to occur before it can bind to an ion at the opposite side (resulting in a cyclic reaction scheme as in the case of an enzyme, closed loops in Fig. 7*A*). Another difference is that binding and unbinding reactions do not sense membrane potential.

For activation and deactivation processes a so-called lazy state had to be incorporated. A lazy state is an inactive state of the transport molecule. The difference from other models with an inactive state is that in the case of the lazy state model the transport molecule can go into the lazy state only from special states of the transport cycle (Hansen, 1990; Hansen et al., 1983; Hansen & Fisahn, 1987). The lazy state leads to a difference between the models which might be revealed by an experimental approach: The Hille-Schwarz model can generate the anomalous mole fraction effect by an influence on the open-channel conductivity. However, the open-channel conductivity should remain unchanged in the enzyme-kinetic lazy-state model, but the transitions into and out of the lazy state should become obvious if open probability of the channel is investigated. The distinction between open-channel conductivity and open probability requires a patch-clamp approach. Experiments dealing with single channel recordings in cytoplasmic droplets of *Nitella* are reported here.

Materials and Methods

Nitella flexilis was bought from R. Kiel, Frankfurt, and kept in artificial pond water (APW: 0.1 mM KCl, 1.0 NaCl, 0.1 $CaCl_2$) at 18°C in a refrigerator at a light intensity of 2 W m^{-2} (12 hr/day). For the isolation of cytoplasmic droplets, the cells were taken out of the basin and were exposed to air for about 2–3 min in order to induce wilting. Then cells were cut, and a droplet formed at the open end after gentle squeezing. This droplet was released into a Petri dish containing the experimental solution composed of 150 mM (KNO_3 plus $TLNO_3$) and 10 mM $Ca(NO_3)_2$. The same solution was used for filling the pipettes. For the analysis of the anomalous mole fraction effect, *I-V* curves were measured at seven different mixtures of Tl^+/K^+. The sum of the concentration of monovalent cations was 150 mM. :NO_3^- served as a counterion. 10 mM $Ca(NO_3)_2$ was used in order to support sealing. A problem was that in high Tl^+ solutions the droplets often tended to swim rather than to attach to the glass bottom. According to Bertl (1989), Lühring (1986) and Sakano and Tazawa (1986) these droplets consist of inside-out tonoplast fragments.

Patch electrodes were pulled from borosilicate glass (AR-type, Hilgenberg, Malsberg, FRG) by a L/M-3P-A-puller (List-Electronic, Darmstadt). Fire polishing was done in the first experiments, but was found not to be necessary. The electric resistance of the patch electrodes was about 9 to 12 MΩ. A patch-clamp amplifier EPC-7 (List) was used for electrical recording. The preamplifier was mounted on a hydraulic Narishige (Tokyo) manipulator, and the attachment of the electrode to the membrane was observed by an inverse microscope (ID 02, Zeiss, Oberkochen). An agar bridge was used to connect the bathing medium to the ground Ag/AgCl-electrode.

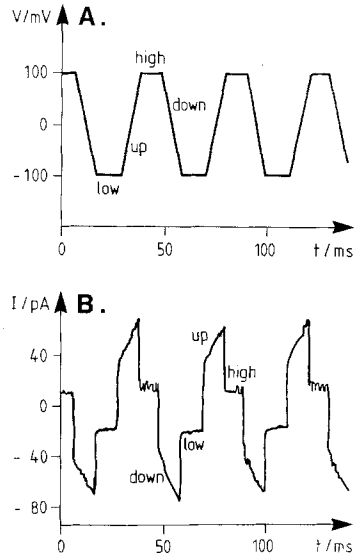

Fig. 1. (*A*) Command voltage signal applied to the EPC-7 consisting of four phases each 10 msec long. (*B*) Patch current as induced by the command voltage in *A*. *Nitella* droplet was in solution containing (in mM) 50 KNO_3, 100 $TlNO_3$, and 10 $Ca(NO_3)_2$

For the measurement of *I-V* curves, a protocol similar to that of Tyerman and Findlay (1989) was employed. Periodic ramp functions with equal upward and downward slopes and plateaus in between were used as a command voltage for the EPC-7 (Fig. 1*A*). Each segment of the signal had a length of 10 msec, thus giving an overall period of 40 msec. The short period of 40 msec prevented the K^+ channel, a delayed outward rectifier, from closing at hyperpolarizing potentials, at least during the down ramp.

The resulting current signal is shown in Fig. 1*B*. After low-pass filtering (1 kHz), the signal was fed into a pulse code modulator (Sony PCM-601 ESD) and stored digitally on a VHS video recorder (Bezanilla, 1985). Transfer to the XT-compatible computer was done via a laboratory-made handshake unit at a sampling rate of 3 kHz. Data evaluation on the computer by a program written in Turbo Pascal is described in Results.

Results

Measurements were done in the cell attached configuration (Hedrich & Schroeder, 1989) as this technique yielded more stable seals in Tl^+ solutions. Stable seals were required for the time-consuming

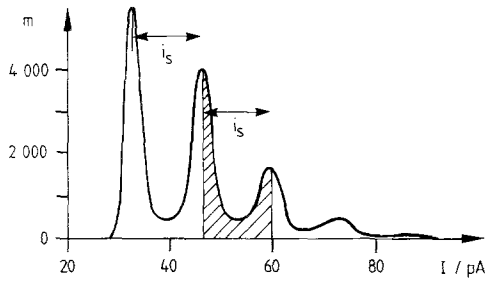

Fig. 2. Histogram of currents measured in the high phase of Fig. 1*A* at (the rarely applied potential of) +200 mV. 360,000 records were taken. The solution was in 150 mM KNO_3 + 10 $Ca(NO_3)_2$. The distance between the peaks yields the apparent open-channel current i_s. The hatched area is used for the determination of open probabilities [Eq. (A2)]. m = number of records

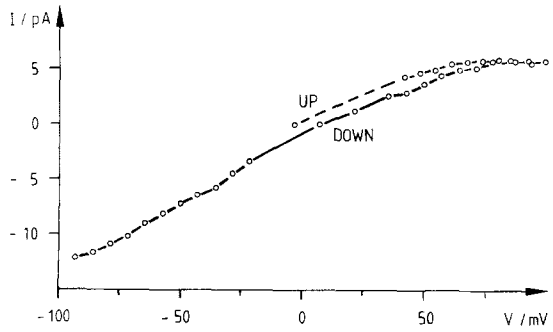

Fig. 3. Current-voltage curve as obtained from an upward and a downward ramp of command voltage (Fig. 1). Apparent open-channel current is determined from the distance between peaks as in Fig. 2. The bathing medium was 150 mM KNO_3, 10 mM $Ca(NO_3)_2$. The upward curve begins in the middle because open probability is very small after hyperpolarization

measurements of *I-V* curves. In addition, Laver, Fairley and Walker (1989) have found for similar K^+ channels in *Chara* that the conductance obtained from excised patches differs from those obtained in the cell-attached mode. As our investigations deal with the anomalous mole fractions effect observed in intact cells the cell-attached configuration may be a more adequate approach. Unfortunately, the cell-attached technique does not provide the real membrane potential of the patch under the electrode. Thus, the expression "membrane voltage" (V) refers to the potential difference between the inside of the pipette and the outside of the droplet. However, membrane potential of the vesicle is assumed to be about zero because the high ion concentrations in the bathing medium are assumed to short circuit the vesicle.

The command signal described above (Fig. 1*A*) was employed, and the resulting current signal was recorded (Fig. 1*B*). Switching of channels can be observed at the horizontal parts. The response of the slopes consists of a large capacitive current superimposed by the current of the open channels.

The ramps ranging from −100 to +100 mV were divided into intervals of 5 mV, and histograms (Fig. 2) of the measured current were generated for each of these intervals. From these histograms the current i_s of a single open channel was determined by visual inspection from the distance between the peaks (*see* horizontal bars in Fig. 2). Three to five peaks could be identified (indicating that several channels were in the patch) and were used for the determination of single open-channel current by linear regression. Plotting the open-channel currents *versus* voltage resulted in current-voltage curves (*I-V* curves). Figure 3 shows data from the upward ramp plus data from the downward ramp. Hysteresis is found to be small. The upward data begin in the

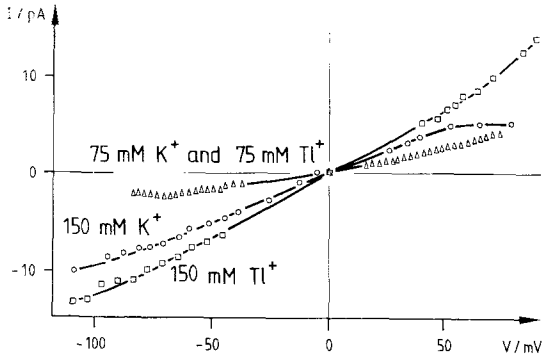

Fig. 4. Current-voltage curves of apparently open channels measured at three different Tl^+/K^+ ratios as indicated in the figure. The reversal potential which was about ± 10 mV is normalized to be zero, first because the cell-attached configuration does not allow its correct determination and second in order to demonstrate the rotation of the I-V curves

middle of the graph because open probability is nearly zero after hyperpolarization, and thus the ensemble of data for a significant analysis is too small. The *I-V* curve in Fig. 3 shows saturation at positive and negative potentials, as expected for a transporter described by a single-barrier enzyme-kinetic model (Hansen et al., 1981).

The investigation of the anomalous mole fraction effect was based on the measurement of *I-V* curves at seven different mixtures of Tl^+/K^+. The sum of the concentrations of monovalent cations was 150 mM. Figure 4 shows three *I-V* curves as obtained in pure K^+ solution, pure Tl^+ solution and in a mixed solution. The smaller conductivity in the mixed solution is obvious. One feature is important: the slope changes in the whole voltage range from −100 to about +80 mV.

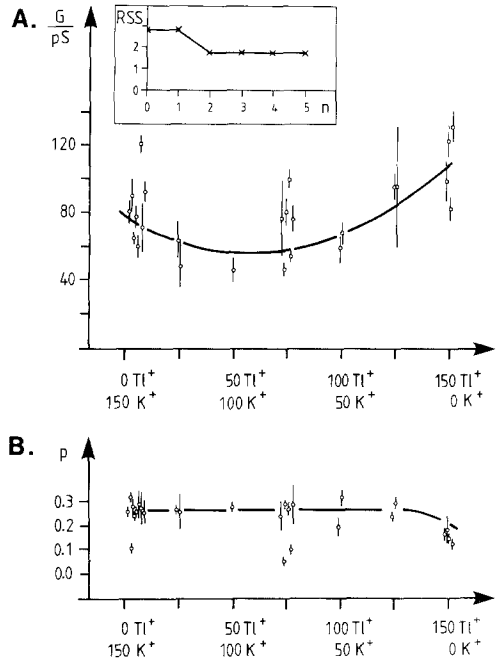

Fig. 5. (*A*) Dependence of apparent open-channel conductance G on Tl^+/K^+ ratio as obtained from the straight slopes in Fig. 4. $[K^+] + [Tl^+] = 150$ mM. The smooth line is obtained from a weighted least-squares fit with a second order polynomial. The weights are inversely proportional to the variances indicated by the error bars. These error bars present 99%-confidence intervals as obtained from the least square fit of a straight line through the straight part of the I-V curves in Fig. 4. Inset: Dependence of the fit error *RSS* (weighted residual sum of squares) on the order n of the polynomial. (*B*) Dependence of apparent open probability P on Tl^+/K^+ ratio as obtained from the areas in Fig. 2 evaluated by Eq. (A4). $[K^+] + [Tl^+] = 150$ mM. Open probability was determined by averaging the nearly constant open probabilities between 0 and -100 mV. The error bars give the scatter of the open probabilities in this range (68% confidence)

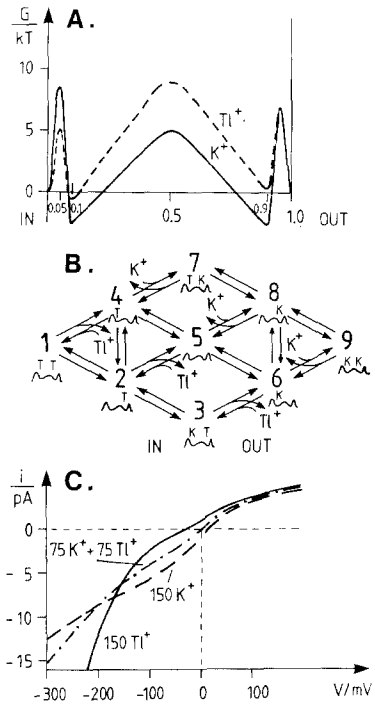

Fig. 6. (*A*) Energy profile of the Hille-Schwarz pore used for the calculations for the curves in *C*. Repulsion factors $1/F_{in} = F_{out} = 30$, $Q = 3 \times 10^{10}$ sec^{-1} (*see* Hille & Schwarz, 1978.) (*B*) Hille-Schwarz model used for the calculations of the *I-V* curves in *C*. (*C*) Typical set of current-voltage curves as calculated from a Hille-Schwarz model displaying the anomalous mole fraction effect of the current in a limited voltage range around -200 mV and of the conductivity (slopes) around -100 mV

Apparent open-channel conductance was determined from the straight slopes of curves like those in Fig. 4. Plotting the conductance *versus* the Tl^+/K^+ ratio shows a minimum conductance at about 60 mM Tl^+ and 90 mM K^+ (Fig. 5*A*). The upper points at 75 mM Tl^+ and 75 mM K^+ seem to weaken this statement. However, the error bars show that these data points result from less reliable experiments. The minimum is clearly indicated by the inset of Fig. 5*A*. Increasing the order of the polynomial used for fitting the data in Fig. 5*A* from one (straight line without a minimum) to two (parabola with minimum, smooth line in Fig. 5*A* gave a significant decrease of the error sum. In addition, the significance was shown by the application of an *F*-test for order selection (Nollau, 1979; Sachs, 1984). Thus, the anomalous mole fraction effect was observed in the apparent open-channel conductance.

Apparent open probabilities were also determined from the histograms shown in Fig. 2. They were calculated by a curve-fitting routine which is described in Appendix A. Figure 5*B* shows that open probability is constant over nearly the whole range of concentration ratios. At least there is no minimum at those ratios, which show the anomalous mole fraction effect.

Discussion

According to the enzyme kinetic lazy-state model described in the introduction, it was expected that the anomalous mole fraction effect should not show up in the single channel conductivity (Fig. 5*A*), but in the open probability (Fig. 5*B*). However, the above investigations yield the opposite results. Therefore, the multi-ion single-file pore model seems to be favored by the data in Figs. 5*A* and *B*.

In order to test this hypothesis, calculations were made on the basis of models like that in Fig.

6*A* and *B*. However, modelling on the basis of the Hille-Schwarz model turned out to suffer from a severe problem: the single-file multi-ion pore model could not create a feature which is very obvious in the measured *I-V* curves in Fig. 4. The slope of the *I-V* curves changes with the K^+/Tl^+ ratio without cross-over (except at the reversal potential) in the whole voltage range. Unfortunately, we cannot give a general proof. However, we did numerous computer simulations on the basis of the Hille-Schwarz model. Even though the model has many parameters like positions and heights of energy barriers and repulsion factors, which result in 17 essential parameters for a two-site model, we got the impression that the simulations showed the crucial features: The majority of simulations created just a monotonous dependence on the K^+/Tl^+ ratio. Only some rare sets of parameters resulted in current-voltage relationships similar to that shown in Fig. 6*C*. In the range with membrane potential more positive than -100 mV the K^+ influx is more dominant than the Tl^+ influx. In the range of potentials more negative than -250 mV the Tl^+ influx is greater. In both ranges the current depends monotonously on the K^+/Tl^+ ratio. Only in the narrow "cross-over" region between -220 and -180 mV the current depends "anomalously" on the Tl^+/K^+ ratio, i.e., the conductivity of a mixed solution was found to be smaller than those of pure solutions. In none of the simulations could we create *I-V* curves like those in Fig. 4 on the basis of the Hille-Schwarz model. Hille and Schwarz (1978) themselves pointed out that a cross-over of the *I-V* curves is a characteristic feature of their model.

Thus, the enzyme-kinetic model with lazy-state was used for modelling again. Theoretical considerations led to some rules by means of which adequate models could be selected. One important feature is that there must be at least one line segment pointing to a certain state in the King-Altman (1956) scheme, which comprises two ion-binding reactions in order to create a nonmonotonous dependence (at least quadratic) of transport rate on ion concentrations (Appendix B).

The configuration shown in Fig. 7*A* results in *I-V* curves (Fig. 7*B*) similar to those in Fig. 4. Plotting the conductivity as obtained from the straight slopes of Fig. 7*B* *versus* Tl^+/K^+ ratio displays the anomalous mole fraction effect (Fig. 7*C*) as observed in Fig. 5*A* or in whole cell measurements (Tester, 1988; Hagiwara et al., 1977).

The channel in Fig. 7*A* has two binding sites for K^+. One is the transport binding site, which can be occupied by K^+ or Tl^+ as indicated by the black ball in the pore. The other one is given by the pocket at the right-hand side of the pore. This regulatory

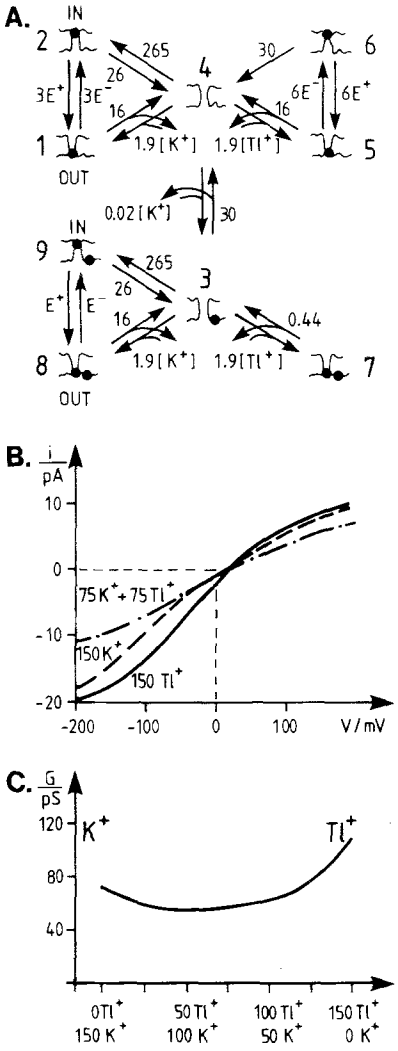

Fig. 7. (*A*) Enzyme kinetic lazy-state model with a single transport site for K^+ or Tl^+ (indicated by the black ball in the pore) with a regulatory site (indicated by the pocket at the right-hand side of the pore) which binds selectively to K^+. The rate constants are given in units of 10^7 sec^{-1}. $E^+ = \exp(V/V_b)$, $E^- = \exp(-V/V_b)$, $V_b = 52$ mV, Inside concentrations of $K^+ = 80$ mM and of $Tl^+ = 0$ mM. (*B*) Average current-voltage curves calculated from the model in *A* with the indicated rate constant for three different Tl^+/K^+ ratios as indicated in the figure. (*C*) Dependence of averaged conductance on Tl^+/K^+ ratio as obtained from the straight slopes in *B*. $[K^+] + [Tl^+] = 150$ mM

binding site is assumed to be very specific. It can bind to K^+ only. If the regulatory binding site is unoccupied, the transporter can transport K^+ or Tl^+. However, if the regulatory binding site is occupied by K^+, the configuration of the channel is modified in such a way that Tl^+ can no longer be transported. Instead, it blocks the channel. This behavior creates a lazy state (Fig. 7*A*, 7), which will withdraw transporters from the transport cycle only if both ions, K^+ and Tl^+, are present.

The model of Fig. 7*A* yields a good description of the measured *I-V* curves, but it includes a feature that seems to be a crucial contradiction against the experimental findings shown in Figs. 5*A* and *B*: a lazy-state model should modulate transport rate via transitions into and out of the lazy state (Fig. 7*A*). This ought to modulate the open probability and leave the open-channel current unchanged. The only way out of this problem is the assumption that the exchange with the lazy state is much faster than 1 msec. In that case, these open-close transitions cannot be observed with the temporal resolution of our recording apparatus. Instead, the apparent open-channel conductance would be changed as it results from an average over undetected open-close states. A similar assumption has been made in the case of blockade by Na^+ of the K^+ channel in *Chara* (Bertl, 1989).

The model of Fig. 7*A* is hypothetical. Experimental evidence for its existence is poor. Nevertheless, there are results from other authors that indicate at least the existence of a regulatory K^+ binding site. Blatt (1988) has found K^+-dependent gating of K^+ channels in guard cells. Mechanisms of a related type may be indicated by the control of transport activity by phosphorylation at the serine residues of H^+-ATPases (McDonough & Mahler, 1982; Portillo & Mazon, 1985; Kolarev et al., 1988), by the existence of a "modulation site outside the ion-conducting pore" of cyclic AMP-stimulated K^+ channels from rat pancreas (Gray et al., 1990), or by altered ion selectivity of Na^+ channels modified by aconitine (Negulyaev, Vedernikova & Savokhina, 1990). The special assumption of the model in Fig. 7*A* is that such a regulatory site can influence the specificity of the transport site in such a way that Tl^+ blocks the pore if K^+ is bound to this site. This mechanism is similar to that proposed for the influence of a H^+-binding site on the dihydropyridine-sensitive Ca^{2+} channel (Prod'hom, Pietrobon & Hess, 1987). Binding of protons to this allosteric site leads to conformational changes of the protein which alter channel conductivity by a factor of 3. (Their "lazy state" is a little more busy than that postulated here.) The deprotonation rate constant can be influenced by the permeant ion (Pietrobon, Prod'hom & Hess, 1988). The authors suppose that such a mechanism may provide an explanation for the anomalous mole fraction effect without assuming a multi-ion pore. Something like a lazy state is incorporated into a Hille-Schwarz model of the gramicidin A channel by Heinemann and Sigworth (1990). Modulation of channel conductivity is brought about by fluctuating barrier heights for ion entry. Their data obtained from the analysis of excess noise excludes changes in the height of the central energy barrier. Also in the case of our results we doubt that changes in the central energy barrier are involved. The changes in the *I-V* curves in Fig. 4 are similar to those induced by changes in temperature (Hansen & Fisahn, 1987) and or light (Hansen et al., 1989) in intact cells of *Nitella*. In those experiments a lazy state model gave a good fit of the (probably Ca^{2+}-mediated, Vanselow & Hansen, 1989) effect of photosynthesis on the K^+ channel, whereas fits failed completely when they were based on the assumption that height of energy barrier of the translocation step changes.

Further research should try to improve the temporal resolution in order to observe the transitions into and out of the lazy state. This could be accomplished in the case of Cs^+ blockade of the K^+ channel in *Chara* (H.G. Klieber and D. Gradmann, *personal communication*).

These investigations were supported by the Deutsche Forschungsgemeinschaft (Ha 712/7-5). We are grateful to Prof. Dr. D. Gradmann and to Dr. H.-G. Klieber, Göttingen, for helpful discussions, to Mr. R. Linke for help with the set-up, and to Mrs. E. Götting for drawing the figures.

References

Bertl, A. 1989. Current-voltage relationships of a sodium-sensitive potassium channel in the tonoplast of *Chara corallina*. *J. Membrane Biol.* **109**:9–19

Bertl, A., Gradmann, D. 1987. Current-voltage relationships of potassium channels in the plasmalemma of *Acetabularia*. *J. Membrane Biol.* **99**:41–49

Bertl, A., Klieber, H.G., Gradmann, D. 1988. Slow kinetics of a potassium channel in *Acetabularia*. *J. Membrane Biol.* **102**:141–152

Bezanilla, F. 1985. A high capacity data recording device based on a digital audio processor and a video cassette recorder. *Biophys. J.* **47**:437–441

Blatt, M.R. 1988. Potassium-dependent, bipolar gating of K^+ channels in guard cells. *J. Membrane Biol.* **102**, 235–246

Fisahn, J., Hansen, U.-P., Gradmann, D. 1986. Determination of charge, stoichiometry and reaction constants from *I-V* curve studies on a K^+ transporter in *Nitella*. *J. Membrane Biol.* **94**:245–252

Goodwin, G.C., Sin, K.S. 1984. Adaptive Filtering Prediction and Control. pp. 505–507. Prentice-Hall, Englewood Cliffs

Gradmann, D., Klieber, H.G., Hansen, U.P. 1987. Reaction kinetic parameters for ion transport from steady-state current-voltage curves. *Biophys. J.* **51**:569–585

Gray, M.A., Greenwell, J.R., Garton, A.J., Argent, B.E. 1990. Regulation of maxi-K^+ channels on pancreatic duct cells by cyclic AMP-dependent phosphorylation. *J. Membrane Biol.* **115**:203–215

Hagiwara, S., Miyazaki, S., Krasne, S., Ciani, S. 1977. Anomalous permeabilities of the egg cell membrane of a starfish in K^+-Tl^+ mixtures. *J. Gen. Physiol.* **70**:269–281

Hansen, U.P. 1990. Implications of control theory for homeostasis and phosphorylation of transport molecules. *Bot. Acta* **103**:15–23

Hansen, U.P., Dau, H., Vanselow, K.H., Fisahn, J., Stein, S., Kolbowski, J. 1989. Thylakoid and plasmalemma fluxes. *In:* Plant Membrane Transport: The Current Position. J. Dainty,

M.I. De Michelis, E. Marrè, and F. Rasi-Caldogno, editors. pp. 345–350. Elsevier, Amsterdam—New York—Oxford

Hansen, U.-P., Fisahn, J. 1987. *I-V*-curve studies of the control of a K^+-transporter in *Nitella* by temperature. *J. Membrane Biol.* **98:**1–13

Hansen, U.P., Gradmann, D., Sanders, D., Slayman, C.L. 1981. Interpretations of current-voltage relationships for "active" ion transport systems: I. Steady-state reaction-kinetic analysis of class-I mechanisms. *J. Membrane Biol.* **63:**165–190

Hansen, U.-P., Tittor, J., Gradmann, D. 1983. Interpretation of current-voltage relationships for "active" ion transport systems: II. Nonsteady-state reaction-kinetic analysis of Class-I mechanisms with one slow time-constant. *J. Membrane Biol.* **75:**141–169

Hedrich, R., Schroeder, J.I. 1989. The physiology of ion channels and electrogenic pumps in higher plants. *Annu. Rev. Plant Physiol.* **40:**539–569

Heinemann, S.H., Sigworth, F.J. 1990. Open channel noise: V. Fluctuating barriers to ion entry in gramicidin A channels. *Biophys. J.* **57:**499–514

Hille, B., Schwarz, W. 1978. Potassium channels as multi-ion single-file pores. *J. Gen. Physiol.* **72:**409–442

King, E.L., Altmann, C. 1956. A schematic method of deriving the rate laws for enzyme-catalyzed reactions. *J. Phys. Chem.* **60:**1375–1378

Kolarev, J., Kulpa, J., Baijot, M., Goffeau, A. 1988. Characterization of a protein serine kinase from yeast plasma membrane. *J. Biol. Chem.* **263:**10613–10619

Laver, D.R., Fairley, K.A., Walker, N.A. 1989. Ion permeation in a K^+ channel in *Chara australis:* Direct evidence for diffusion limitation of ion flow in a maxi-K channel. *J. Membrane Biol.* **108:**153–164

Lühring, H. 1986. Recording of single K^+ channels in the membrane of cytoplasmic drop of *Chara australis. Protoplasma* **133:**19–28

McDonough, J.P., Mahler, H.P. 1982. Covalent phosphorylation of the Mg^{2+}-dependent ATPase of yeast plasma membranes. *J. Biol. Chem.* **257:**14579–14581

Negulyaev, Yu.A., Vedernikova, E.A., Savokhina, G.A. 1990. Aconitine-induced modification of single sodium channels in neuroblastoma cell membrane. *Gen. Physiol. Biophys.* **9:**167–176

Nollau, V. 1979. Statistische Analysen. Birkhäuser, Basel—Stuttgart

Pietrobon, D., Prod'hom, B., Hess, P. 1988. Conformational changes associated with ion permeation in L-type calcium channels. *Nature* **333:**373–376

Portillo, F., Mazon, M.J. 1985. Activation of yeast plasma membrane ATPase by phorbol ester. *FEBS Lett.* **192:**95–98

Prod'hom, B., Pietrobon, D., Hess, P. 1987. Direct measurement of proton transfer rates to a group controlling the dihydropyridine-sensitive Ca^{2+} channel. *Nature* **239:**243–246

Sachs, L. 1984. Applied Statistics. Springer-Verlag, New York—Berlin—Heidelberg—Tokyo

Sakano, K., Tazawa, M. 1986. Tonoplast origin of the envelope membrane of cytoplasmic droplets prepared from *Chara* internodal cells. *Protoplasma* **131:**247–249

Sorensen, H.W. 1980. Parameter Estimation. pp. 183–199. Marcel Dekker, New York—Basel

Tester, M. 1988. Potassium channels in the plasmalemma of *Chara corallina* are multi-ion pores: Voltage-dependent blockade by Cs^+ and anomalous permeabilities. *J. Membrane Biol.* **105:**87–94

Tyerman, S.D., Findlay, G.P. 1989. Current-voltage curves of single Cl^- channels which coexist with two types of K^+ channels in the tonoplast of *Chara corallina. J. Exp. Bot.* **40:**105–117

Vanselow, K.H., Hansen, U.P. 1989. The rapid effect of light on the K^+ channel in *Nitella. J. Membrane Biol.* **110:**175–187

Received 17 December 1990; revised 26 March 1991

Appendix A

Evaluation of Open Probability

The calculation of the open probability p is based on the assumption that a binomial distribution applies to these data. The sum F_n of the observations of current values between the maxima of n and $(n-1)$ peak in Fig. 2 (corresponding to the area between those peaks) is given by the probability function

$$w(n,p,N) = 0.5\binom{N}{n}p^n(1-p)^{N-n} + 0.5\binom{N}{n-1}p^{n-1}(1-p)^{N-n+1} \tag{A1}$$

with p being the open probability, N the total number of channels under the patch electrode. A first estimate of N is taken from the number of peaks in histograms like those of Fig. 2. This estimate can be improved by repeating the following calculations for increasing numbers of N and using a Chi-Square test (Nollau, 1979; Sachs, 1984) for the selection of the optimum value.

The sum F_n of observations between the peaks is chosen because Fig. 2 shows that the distributions related to neighboring peaks overlap. However, it seems to be reasonable to assume that a distribution related to the nth peaks does not significantly extend beyond the middle of $(n+1)$ or $(n-1)$ peak.

The technique of the maximum likelihood approach makes use of the logarithm of the likelihood function L (Sorensen, 1980; Goodwin & Sin, 1984).

$$\ln L(F_o, \ldots F_{N+1}, p, N) = \sum_{n=0}^{N+1} F_n \ln w(n,p,N). \tag{A2}$$

The maximum likelihood estimation of the open probability p is obtained from the zero of the derivative

$$\frac{d\ln L(F_o, \ldots F_{N+1}, p, N)}{dp} = \sum_{n=0}^{N+1} \frac{F_n}{w(n,p,N)} \frac{d\,w(n,p,N)}{dp}. \tag{A3}$$

Introducing Eq. (A1) into Eq. (A3) results in

$$\sum_{n=0}^{N+1} F_n \frac{\frac{(n-1)n}{p^2} - \frac{(N-n)(N+1-n)}{(1-p)^2}}{\frac{n}{p} + \frac{N+1-n}{(1-p)}} = 0. \tag{A4}$$

The value of p which gives a maximum of the likelihood function is determined by an iterative approximation of the zero of the derivative.

As mentioned above, this procedure requires two premises: the knowledge of N and the assumption that a binomial distribution applies. Improving the estimate of N can be combined with the test of the applicability of the binomial distribution. Theoretical values of F_o to F_{N+1} are calculated from the assumed value of N and of p as calculated from Eq. (A4). These theoretical values of F_n are compared with those obtained from the histograms, and a Chi-Square test already mentioned above (Nollau, 1979; Sachs, 1984) is employed. This procedure is repeated for different values of N in order to determine that value of N which gives an optimum fit.

Appendix B

Criterion for Nonmonotonous Dependence of Current on Mole Fraction

The electric current through a single transport molecule with a single barrier is (*compare* Fig. 7*A*)

$$I = e \sum_{i,j} (k_{ij} N_i - k_{ji} N_j) \tag{B1}$$

with N_i and N_j being the probabilities of the states adjacent to the charged translocation step(s). e is the elementary charge. In the case of Fig. 7*A* Eq. (B1) becomes

$$I = e(k_{21} N_2 - k_{12} N_1 + k_{65} N_6 - k_{56} N_5 + k_{98} N_9 - k_{89} N_8). \tag{B2}$$

The probabilities of these states can be calculated by means of the King-Altman (1956) algorithm

$$N_i = D_i / D. \tag{B3}$$

Insertion of Eq. (B1) results in

$$I = e \sum_{i,j} (k_{ij} D_i - k_{ji} D_j)/D \tag{B4}$$

with D_i being the sum of all line segments pointing towards state i, and D being the sum of all line segments pointing to all states.

We define

$$k = K^+/(K^+ + Tl^+). \tag{B5}$$

Then, those rate constants involved in K^+ binding depend linearly on k, those involved in binding Tl^+ depend linearly on $(1 - k)$. k_{ij} and k_{ji} are independent of k, as ion-binding sites and voltage-sensitive steps are separated in the single-barrier enzyme-kinetic model of Hansen et al. (1981).

If we assume that one line segment of the King-Altman graph comprises only one ion-binding reaction, I takes the form

$$I = (a + bk)/(c + dk) \tag{B6}$$

with a, b, c, and d being independent of k. Differentiation of Eq. (B6)

$$\frac{dI}{dk} = \frac{bc - da}{(c + dk)^2} \tag{B7}$$

shows that I depends monotonously on k. Thus, the current I cannot display an anomalous mole fraction effect if there is only one ion-binding reaction in a line segment.